



Adsorptive removal of Congo red from aqueous phase using graphene–tin oxide composite as a novel adsorbent

T. Mahmood¹ · U. Noreen¹ · R. Ali¹ · A. Ullah¹ · A. Naeem¹ · M. Aslam¹

Received: 30 October 2020 / Revised: 30 November 2021 / Accepted: 6 December 2021 / Published online: 17 February 2022
© Islamic Azad University (IAU) 2022

Abstract

The main focus of this work was to prepare graphene tin oxide composite as a novel adsorbent for the removal of hazardous anionic dye, Congo Red, from aqueous systems. The composite was prepared by a simple solvothermal method. The adsorbent was characterized via scanning electron microscopic analysis, energy-dispersive spectroscopy, X-ray diffraction, Fourier transform infrared spectroscopy and thermogravimetric analysis. The energy-dispersive spectra of graphene tin oxide composite showed a high percentage of tin (62.11%) with a reduction in the percentage of carbon (47.45 to 13.75%) and oxygen (39.37 to 23.71%) suggesting that the composite has been successfully prepared. Fourier transform infrared spectroscopic analysis showed that the intensity of some absorption peaks like C=O, C=O and OH decreased which support the effective reduction in graphene oxide to graphene in the composite. Removal of Congo red by graphene tin oxide composite was carried out as a function of pH, dye initial concentration, contact time, temperature and adsorbent dose in batch mode. Optimum adsorption was observed in the pH range of 2 to 4 with contact time of 60 min. Langmuir and pseudo-second order kinetic model fitted very well the isotherm and kinetic data, respectively. The maximum uptake capacity determined by Langmuir model was observed to be 359.71 mg/g at 318 K. Thermodynamic investigations have shown endothermic and spontaneous nature of Congo red adsorption. Regeneration studies revealed that graphene tin oxide composite could be a viable and potential adsorbent for detoxification of dyes bearing wastewater.

Keywords Adsorption · Anionic azo dye · Isotherm models · Kinetic models · Wastewater

Introduction

Water plays a key role in the existence of living organism. Generally, the quantity and quality of water is of main concern around the world. Rapid urbanization, industrialization and population growth have caused a serious problem of water pollution (Madan et al. 2019; Bhat et al. 2020). Various types of toxic substances like pesticides, pharmaceutical residues, heavy metals, drugs and dyes are continuously discharging in water bodies like ocean, lakes and rivers (Basheer 2018). Presently, dyes constitute the most adulterating agents in the effluents from textiles, cosmetic, plastic, rubber, leather, paper and pharmaceutical industries.

Over 0.7 million tons of dyes are produced annually worldwide and almost 12–15% dyes are lost mainly from textile and other dyeing industries which are discharged as effluents in various aqueous environments without any handling (Mahmood et al. 2018; Parvin et al. 2019). The dyes containing effluents lead to many ecological complications. Owing to their intense color and high biological oxygen demand (BOD), dyes bearing effluents decline the photosynthetic activities of various phytoplankton and decrease the required oxygen level of water which leads to oxygen deprivation of aquatic fauna and flora and results in suffocation (Deng et al. 2018; Naushad et al. 2019a). Dyes, particularly azo dyes due to their recalcitrant molecules are high stable, non-biodegradable and exist for longer time in environment. Congo Red (CR) is an anionic azo dye, present in effluent from textile and other industries. It is highly toxic, causes allergies, skin irritation and is considered as carcinogenic and mutagenic for human beings (Aliabadi and Mahmoodi 2018; Wekoye et al. 2020). Therefore, there has been an

Editorial responsibility: Ta Yeong Wu.

✉ T. Mahmood
tahiramahmood@uop.edu.pk

¹ National Center of Excellence in Physical Chemistry,
University of Peshawar, Peshawar 25120, Pakistan



increasing demand for effective removal of these dyes from water bodies to safeguard human life and the aquatic biota.

Several treatment methods such as precipitation, flocculation/coagulation, electro-dialysis, nano-filtration, photo-chemical degradation, chemical oxidation, aerobic and anaerobic degradation have been applied for the removal of azo dyes from aqueous systems (Golmohammadi et al. 2019; Naushad et al. 2019b; Dbik et al. 2020). Most of these technologies are less effective, have high operation cost, time consuming, and may leads to the formation of some intermediate toxic products which limit their prevalent applications in poor nations (Sun et al. 2011; Yang et al. 2018). But, adsorption due to its simplicity, effectiveness, low cost and ability to purify large quantity of dyes bearing wastewater without production of any harmful by-products is the most promising and frequently used method around the world (Bharath et al. 2017; Deng et al. 2018). Until now, a variety of materials like biomass, silica, polymer gels, organic and inorganic composites, clays, metal–organic framework (MOF) and carbon-based adsorbents have been tested for removal of toxic dye from water bodies (Mahmood et al. 2017; Tang et al. 2020). Recently, numerous carbon skeleton materials like carbon nanotubes, fullerene and graphene exhibited very good removal efficiency for different organic pollutants.

Graphene oxide (GO), a derivative of graphene, has two-dimensional sheet-like carbon structure containing many oxygen functional groups such as carboxyl, hydroxyl, epoxy and carbonyl groups on edges and surface of its lattice (Liu et al. 2019a). The unique physical and chemical structural of GO make it to be highly dispersed in aqueous mediums which can facilitate its interactions with solute molecules via hydrogen bonding and electrostatic interactions and hence make it as a good adsorbent for dyes removal in pollution control applications (Jiao et al. 2016). However, GO sheets due to their high specific surface area have the tendency to agglomerate in liquid phase which leads to a reduction in the number of active sites available for adsorption. This behavior of GO restricts its direct application for pollutants removal from aqueous solutions. To overcome the problem of agglomeration of GO nano-sheets in liquid medium and improve its efficiency for dyes removal, the most convenient strategy is to make composite of GO with different metal oxides, polymers and ionic liquids (Mohammadi et al. 2018; Abbasi 2020).

In the present study, graphene and tin (IV) oxide composites (G/SnO₂) were synthesized and its adsorption capacity was evaluated for the removal of toxic anionic diazo dye, CR from aqueous solutions. Detailed literature survey showed that G/SnO₂ composite has not been used for the adsorption of CR from synthetic wastewater. This study attempts to assess the impact of major process variables such as pH, dye initial concentration, contact time, temperature and

adsorbent dose on CR adsorption by G/SnO₂ composite. Additionally, the correlation between the dye uptake capacity and adsorption mechanism was evaluated with different isotherm and kinetic models by performing systematic equilibrium and kinetic studies.

The research work was carried out in environmental science and Material Chemistry Laboratory at National Center of Excellence in Physical Chemistry, University of Peshawar, Pakistan, Dated 12th June 2019 to 28th December 2019.

Materials and methods

Chemical and reagents

Analytical grade chemicals/reagents were used in the present study without further purification. Graphite powder, potassium permanganate (99.0%), HCl (37%), hydrogen peroxide (30%), NaOH (99.99%) and acetone (99.90%) were purchased from Scharlau, Spain. Anionic dye Congo red (95%) and Tin (II) chloride dehydrate (99.99%) was purchased from Sigma Aldrich, Germany. Fresh double distilled water (DDW) was used all over the experimental work. The various characteristics and structure of CR are given in Table 1. CR dye solutions of desired initial concentration were prepared by diluting its stock solution (1000 mg/L) with DDW.

Adsorbent preparation

Synthesis of GO

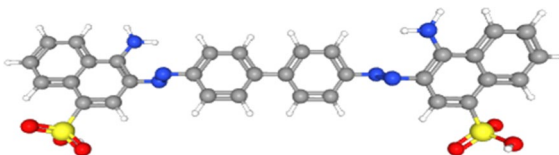
GO was synthesized via modified Hummers method (Alam et al. 2017). First 2.0 g graphite powder was put in 100 mL of concentrated H₂SO₄ at 0 °C. Then, 8.0 g of KMnO₄ was added slowly with continuous stirring for 2 h below 10 °C. The temperature of the reaction mixture was then raised to 35 °C and further stirred at this temperature for 1 h. DDW was then added to the reaction mixture below 100 °C and again stirred for 1 h which is then followed by addition of 300 mL DDW. After this 20 mL H₂O₂ was added to the mixture for the reduction in residual KMnO₄ which turned yellow. The resulting graphene oxide sample was washed first with 5% HCl solution and then with 1 L of DDW for removing the acid. The GO was then dried in an oven at 60 °C for 24 h.

Synthesis of G/SnO₂ composite

Graphene tin oxide composite (G/SnO₂) was prepared by Solvothermal method (Wu et al. 2010). In a typical procedure 0.04 g of GO, prepared by modified Hummers method, was dispersed in 20 mL ethanol through ultra-sonication process for 90 min to get solution A. Solution B was obtained by

Table 1 Important physical properties and structure of Congo Red

C.I name	Direct Red 28
Commercial name	Congo Red
Abbreviation	CR
IUPAC name	Disodium; 4-amino-3-[[4-[4-[(1-amino-4-sulfonatophthalene-2-yl)diazonyl]phenyl]phenyl]diazonyl]naphthalene-1-sulfonate
Molecular formula	C ₃₂ H ₂₂ N ₆ Na ₂ O ₆ S ₂
Molar mass (g/mol)	696.66
C.I No	22,120
Chemical class	Anionic
Ionization	Acidic
Color	Red (above pH5.2), blue (below pH3.0)
Solubility in H ₂ O	10 g/L at 20 °C
λ _{max} (nm)	498
Structure	



dissolving 0.25 g tin chloride dihydrate in 20 mL absolute ethanol. Solution A and B were mixed and shifted to autoclave and kept in the oven for 10 h at 160 °C. The autoclave was then allowed to cool down and the product obtained was washed several times through centrifugation process followed by drying at 60 °C to get G/SnO₂.

Adsorbent characterization

GO and G/SnO₂ composite was characterized by various physicochemical techniques. Morphological examinations were carried out using a JEOL, JSM-5910 scanning electron microscope (SEM) with 20 kV accelerating voltage and resolution of 3.0 nm. Elemental compositions were evaluated by energy-dispersive spectroscopic (EDS) micro-analyzer (EDX Inca-200, UK) coupled with SEM analyzer. XRD analysis was performed to observe the crystalline nature of GO and G/SnO₂ using X-ray diffractometer (JEOL, model JDX-3532) with Mn filtered Cu-Kα radiations. XRD patterns were taken in the range of 10°–80° (2θ) with step size of 0.04° and a step time of 0.5 s. The applied current and voltage were kept at 30 mA and 40 kV, respectively. The chemical structure and surface functional groups were analyzed using Fourier Transform Infrared (FTIR) spectrophotometer (FTIR-8201PC 2000, Shimadzu) in the range of 500–4000 cm⁻¹. Prior to FTIR analysis GO and G/SnO₂ were mixed with KBr powder and the mixture was homogenized thoroughly. Thermal stability of GO and G/SnO₂ was evaluated in the temperature range of 20–1000 °C at a heating rate of 10 °C/min using Perkin-Elmer Pyris1 analyzer, model 6300. Point of zero charge (PZC) was determined via a well-defined drift method (Ali et al. 2019).

Adsorption studies

Adsorption of CR by G/SnO₂ composite was carried out in batch mode by considering the impact of various processes variables such as solution pH, dye initial concentration, contact time, temperature and adsorbent dose. A fixed amount of adsorbent (0.1 g) was put in 40 mL of dye solution of desired concentration taken in a series of polythene bottles (100 mL capacity) and agitated in a shaker bath (SHEL LAB, WS 17-2, USA) at 120 rpm at definite temperature for a desired time interval. The pH of dye solution was adjusted via 0.1 M HCl or/and NaOH solution using a pH meter (Neo Met, pH 250 L, Korea). At the end of saturation point the dye solutions were filtered and analyzed for the left over concentration of CR at the wavelength of 498 nm using Vernier SpectroVis® Plus (SVIS-PL) spectrophotometer. The adsorption capacity q_e (mg/g) and removal efficiency (%R) were determined from the following equations:

$$q_e = \frac{V(C_o - C_e)}{m} \quad (1)$$

$$\%R = \frac{(C_o - C_e)}{C_o} \times 100 \quad (2)$$

where C_o and C_e are the dye concentrations (mg/L) in solution before and after adsorption, respectively, V is the volume (L) and m (g) is the mass of adsorbent.



Equilibrium isotherm study

Adsorption isotherm experiments were performed by contacting 40 mL of CR dye solutions (20–1000 mg/L) with 0.1 g of adsorbent which were taken in a series of 100-mL bottles with their pH adjusted at 3.0 and shaken at constant temperature (298, 308 and 318 K) in a shaker bath at 120 rpm until the point of equilibrium is achieved. After filtration, the concentration of the residual dye solutions was measured spectrophotometrically at the wavelength of maximum absorption ($\lambda_{\max} = 498$ nm). In the current study the experimentally obtained isotherm data were analyzed via Freundlich, Langmuir and Temkin models.

Freundlich isotherm equation is an empirical model for adsorption on heterogeneous surfaces which assumes multilayer, reversible and non-ideal adsorption due to non-uniform distribution of adsorption sites. The linear form of Freundlich isotherm equation can be represented (Freundlich 1907; Al-Othman et al. 2012) as:

$$\ln q_e = \ln K_F + \frac{1}{n} \ln C_e \quad (3)$$

where K_F (mg/g (L/mg)^{1/n}) is Freundlich constants correspond to adsorption capacity, while n is known as heterogeneity factor that shows the adsorption intensity.

Langmuir isotherm model is based on the assumption that all the binding positions on adsorbent surface are fixed and homogeneous which leads to monolayer adsorption. The mathematical linear form of Langmuir isotherm equation is written (Langmuir 1916) as:

$$\frac{C_e}{q_e} = \frac{1}{K_L q_m} + \frac{C_e}{q_m} \quad (4)$$

where q_e and q_m refer to the amount of CR adsorbed per unit mass of adsorbent and monolayer adsorption capacity (mg/g), respectively, while K_L (L/mg) denotes the binding energy constant.

The favorability of Langmuir isotherm model for CR adsorption onto G/SnO₂ was further investigated by a dimensionless equilibrium parameter, named as separation factor (R_L) which can be expressed as follows as:

$$R_L = \frac{1}{1 + K_L C_o} \quad (5)$$

where C_o (mg/L) and K_L are the dye initial concentration and the Langmuir binding energy constant, respectively. In case, $0 < R_L < 1$ shows favorable adsorption, $R_L > 1$ unfavorable, $R_L = 1$ linear and $R_L = 0$ indicate irreversible adsorption process (Weber and Chakravorti 1974).

Temkin isotherm model proposes that for all molecules adsorption energy decreases linearly with surface coverage due to adsorbate–adsorbent interactions. The general form

of this isotherm model can be written (Temkin and Pyzhev 1940) as:

$$q_e = \frac{RT}{b_T} \ln K_T C_e \quad (6)$$

$$q_e = \frac{RT}{b_T} \ln K_T + \frac{RT}{b_T} \ln C_e \quad (7)$$

$$q_e = B_T \ln K_T + B_T \ln C_e \quad (8)$$

where T (K) is absolute temperature, R (8.314 J mol⁻¹ K⁻¹) is universal gas constant, while K_T (L/g) is the equilibrium constant, depicts the highest binding energy and b_T (J/mol) is associated with heat of adsorption.

Kinetic study

Adsorption kinetics tests were carried out to examine the impact of contact time and temperature on the CR uptake by G/SnO₂ and to find out the kinetic parameters. A known amount of adsorbent (0.1 g) was contacted with 40 mL of CR dye solution (700 mg/L) in an array of 100-mL polythene bottles at constants solution pH (3.0) and shaken in an isothermal shaker bath for certain time (5–240 min) at 120 rpm at fixed temperature (298, 308 and 318 K). Bottles were withdrawn at definite time intervals from shaker bath, filtered and analyzed for the remaining concentration of CR in the filtrate.

In the present work, the kinetics and mechanism of CR were studied using pseudo-first order (Corbett 1972), pseudo-second order (Ho 2006) and intra-particle diffusion (Weber and Morris 1963) models. The linear form of pseudo-second order kinetic model is expressed as:

$$\log (q_e - q_t) = \log q_e - \left(\frac{k_1}{2.303} \right) t \quad (9)$$

where q_e and q_t denote the CR uptake capacities (mg/g) by G/SnO₂ at equilibrium and at any time t , respectively, while k_1 (1/min) signifies the pseudo-first-order rate constant.

Pseudo-second order kinetic models proposed by Ho and McKay assume that adsorption of adsorbate species on adsorbent surface occurs by chemical interaction as a result of electron sharing between dye molecules and the functional groups on adsorbent surface. The linear form of pseudo-second order kinetic equation can be represented as follows:

$$\frac{t}{q_t} = \frac{1}{k_2 q_e^2} + \frac{1}{q_e} t \quad (10)$$

where k_2 (g/mg min) is the rate constant for pseudo-second order kinetic model.

As many sorption processes are involved in the movement of adsorbate species from bulk solution into adsorbent surface. Therefore, Weber and Morris intra-particle diffusion model was used to observe the effect of mass-transfer resistance on the adsorption of CR by G/SnO₂ and determine the rate controlling step. According to intra-particle diffusion model, the sorption capacity varies with the square root of time. The linear form of this model can be expressed as:

$$q_t = k_i t^{0.5} + C \quad (11)$$

where k_i represents intra-particle diffusion model rate constant (mg/g min^{0.5}) at a given stage i , while the intercept C is related to the boundary layer thickness (mg/g). The adsorption kinetic data were further explained by Boyd model (Boyd et al. 1947) to confirm the rate determining step in the adsorption of CR. Boyd model equation can be represented as:

$$F = 1 - \left(\frac{6}{\pi^2}\right) \sum_m \left(\frac{1}{m^2}\right) \exp(-m^2 Bt) \quad (12)$$

$$F = \frac{q_t}{q_e} \quad (13)$$

Rearranging the above equation:

$$Bt = -0.4977 - \ln(1 - F) \quad \text{when } F > 0.85 \quad (14)$$

$$Bt = \left[\sqrt{\pi} - \sqrt{\pi - (\pi^2 F/3)} \right]^2 \quad \text{when } F < 0.85 \quad (15)$$

where ' F ' is the fraction of CR adsorbed at any time t , while Bt is a mathematical function of F and m is an integer which defines the solution infinite series.

Thermodynamic investigations

To investigate whether the uptake of CR by G/SnO₂ composite is spontaneous process or not, various thermodynamic parameters such as Gibbs free energy change (ΔG°), enthalpy change (ΔH°) and entropy change (ΔS°) were calculated at 298, 308 and 318 K by using the following equations (Hassan et al. 2020).

$$\ln K_L = -\frac{\Delta H^\circ}{RT} + \frac{\Delta S^\circ}{R} \quad (16)$$

$$\Delta G^\circ = \Delta H^\circ - T\Delta S^\circ \quad (17)$$

where T (K) is the solution temperature, R (8.314 J/mol/K) is the universal gas constant, while K_L (L/mg) is equilibrium

Langmuir constant. The ΔH° and ΔS° values were calculated from the slope and intercept of the linear plot of $\ln K_L$ versus $1/T$.

Calculation of activation energy

Activation energy for the adsorption of CR onto the G/SnO₂ composite was determined using Arrhenius equation as follows (Li and Lin 2019):

$$\ln k_2 = \ln A - \frac{E_a}{RT} \quad (18)$$

where E_a is activation energy (kJ/mol), k_2 is the pseudo-second-order rate constant, A is Arrhenius constant which is temperature independent and R is universal gas constant.

Desorption and regeneration studies

Desorption and regeneration tests were executed by contacting a known amount of dye loaded adsorbent (0.5 g) with desorbing medium (200 mL) followed by agitating for 2 h at room temperature (298 K) under the identical conditions as used in adsorption studies. Subsequently, the concentration of CR desorbed was measured spectrophotometrically and the adsorbent recovered was washed and used again in adsorption of CR in next adsorption–desorption cycle. Desorption efficiency was estimated via the equation as given below (Ali et al. 2021):

$$\text{Desorption efficiency} = \frac{C_d}{C_0 - C_e} \times 100 \quad (19)$$

where C_0 and C_e are CR initial and equilibrium concentrations (mg/L), respectively, while C_d is the dye concentration (mg/L) after desorption.

Results and discussion

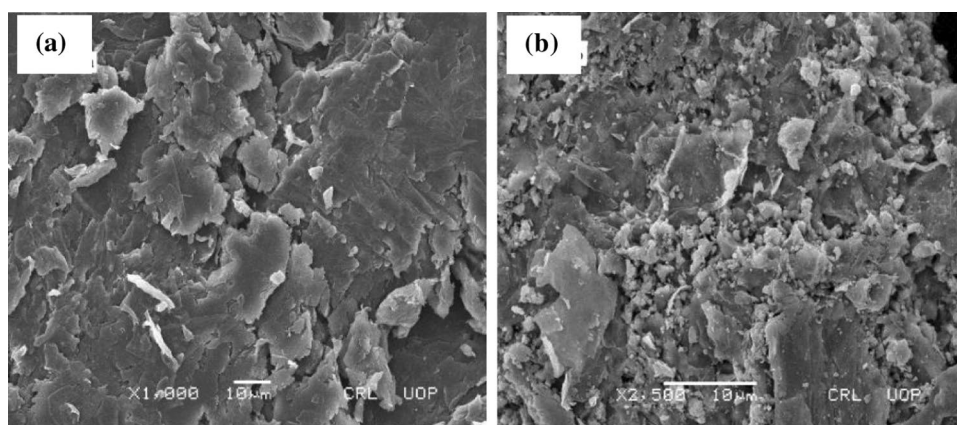
Adsorbent characterization

SEM and EDS analysis

The scanning electron microscope (SEM) images of GO and G/SnO₂ composite are presented in Fig. 1a, b. The SEM image of GO (Fig. 1a) shows irregular porous morphology and un-exfoliated graphene sheets. SEM micrograph of G/SnO₂ composite indicates particles agglomeration and irregular particles morphology as evident from Fig. 1b. Similar observations were made by Dhanabalan et al. (2013) in their study on graphene oxide/tin oxide composite. The percent amount of various elements examined in the EDS spectra of GO and G/SnO₂ composite are given in Fig. 2a, b,



Fig. 1 SEM images of **a** GO and **b** G/SnO₂ composite



respectively. The EDS spectrum of GO contains major peaks for carbon, oxygen and nitrogen and some minor peaks for Na, Mg, Si, Cl and S. The minor peaks indicate the presence of some impurities. The EDS spectrum of G/SnO₂ shows peaks only for carbon, oxygen, Cl and Sn, indicating that the synthesized material is free from impurity and was successfully prepared.

XRD analysis

X-Ray diffraction (XRD) analysis is a worthwhile technique for studying the crystalline nature of solid materials. In the current work, degree of oxidation and crystallography of GO and G/SnO₂ composite was studied using XRD technique and the results obtained are shown in Fig. 3a. In case of GO, a single sharp diffraction peak was observed at 2θ value of about 11.5° which ratifies that the GO was successfully prepared. Same results were also observed by Alam et al. (2017) in the XRD pattern of GO synthesized by modified Hummers method. There are no distinctive peaks in the XRD pattern of G/SnO₂ composite which confirm the amorphous nature of the composite material at 160 °C temperature. The amorphous nature of G/SnO₂ composite at this temperature has been reported in the literature (Lin et al. 2012).

FTIR analysis

Fourier transform infrared (FTIR) spectroscopic technique is commonly used to explore the structure of constituents and the variation in the chemical structure of materials. FTIR spectra of GO and G/SnO₂ composite are given in Fig. 3b. FTIR spectrum of GO displays a wide peak in the range of $3000\text{--}3700\text{ cm}^{-1}$ and a sharp peak at 1713 cm^{-1} , conforming the bending and stretching vibration of OH groups on GO surface. While the existence of absorption peaks, at 1615 cm^{-1} is due to the stretching vibration of C=O and C=C of carbonyl group and carboxylic acid which is present at the corner of GO. The peaks at the 1319 cm^{-1}

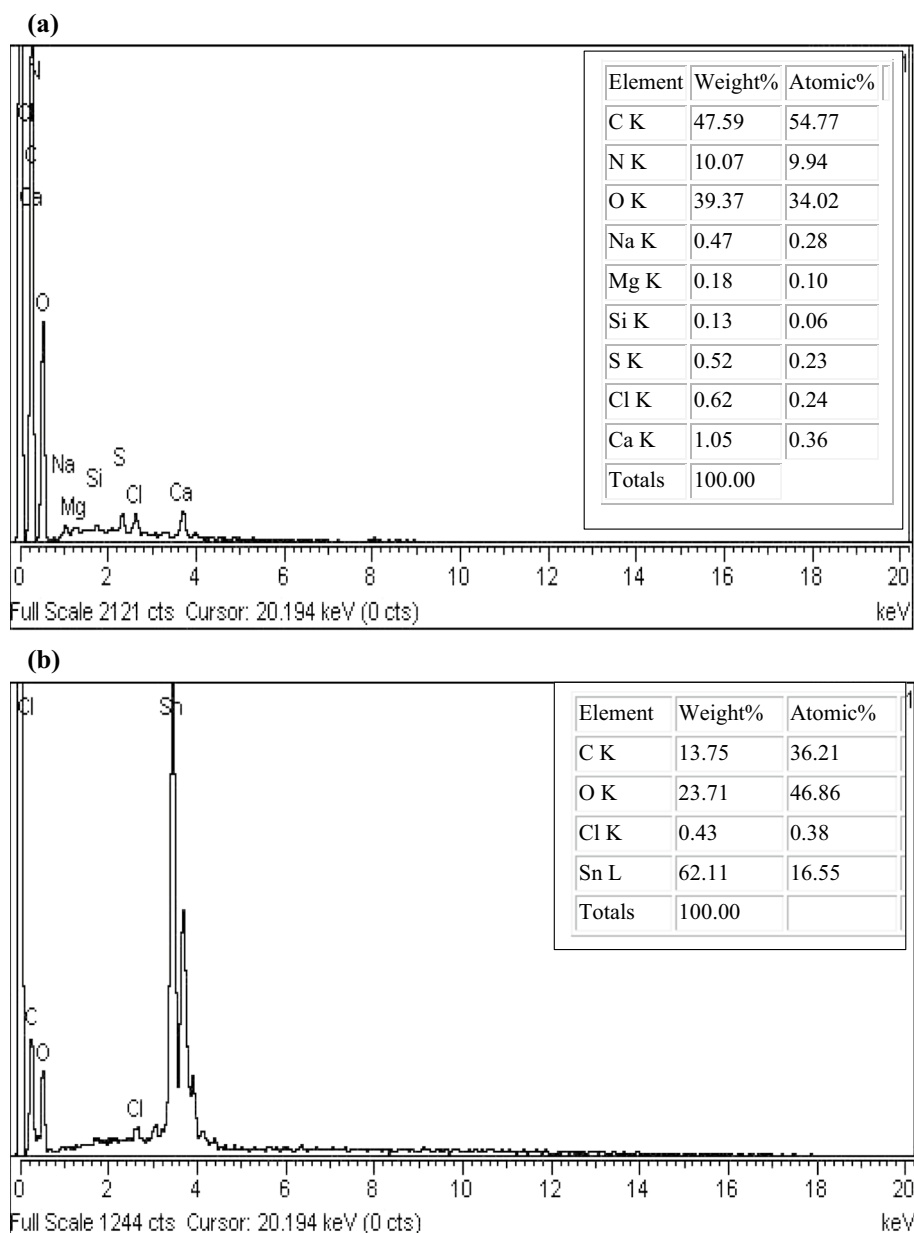
and 1053 cm^{-1} are matching to the stretching vibration of C–OH and C–O of alcohol and carboxylic acid, respectively. The presence of these oxygen containing groups shows the oxidation of graphite into GO (Lin et al. 2012). The FTIR spectrum of G/SnO₂ composite shows shift in intensity of various absorption peaks corresponding to different oxygen containing groups like C=O, C=O and OH, which confirm effective reduction in GO to graphene in G/SnO₂ composite (Zhang et al. 2012).

FTIR spectra of G/SnO₂ composite displayed the occurrence of some new peaks after the adsorption of CR dye. The two sharp peaks that appeared at 1365 cm^{-1} and 1045 cm^{-1} were attributed to the stretching vibration of $-\text{SO}_3$ group and symmetric stretching of S=O, respectively. The new peaks at 1427 and 1180 cm^{-1} correspond to $-\text{N}-\text{H}$ bending and aromatic ring of CR molecules, respectively (Hua et al. 2019). The appearance of new peaks and shifting of some peaks (at 3370 , 1574 , 1218 and 1027 cm^{-1}) to higher wavenumber regions (3456 , 1599 , 1262 and 1045 cm^{-1}) affirming successful adsorption of CR by G/SnO₂ composite.

Thermal analysis

Thermogravimetric (TGA/DTA) study was carried out to find the weight loss of GO and G/SnO₂ composite with rise in temperature. The TGA/DTA plots of GO and G/SnO₂ composite are given in Fig. 3c. As can be seen, GO shows weight loss in three steps. The initial weight loss (18.78%) was observed in the temperature range of $35\text{--}153\text{ }^\circ\text{C}$ and is associated with the removal of water molecules adsorbed on the surface of GO. In the second step a high weight loss (23.63%) was noticed in the temperature of $\sim 200\text{ }^\circ\text{C}$. This change is due to elimination of oxygen containing functional groups like OH, C=O and COOH as carbon monoxide, carbon dioxide and water produced during heat treatment. The third and lost weight loss (40.99%) which occurs in the temperature range of about $430\text{--}550\text{ }^\circ\text{C}$ is associated with the combustion of carbon skeleton of GO. The present finding

Fig. 2 EDS spectra and elemental composition of **a** GO and **b** G/SnO₂



is in close agreement with those reported in the literature (Shahriary and Athawale 2014). The TGA plot of G/SnO₂ composite reveals that the decomposition of carbon skeleton occurred in the temperature range of 480–650 °C, which is much higher than that of graphene oxide. This confirms that G/SnO₂ composite is thermally more stable than GO.

Point of zero charge (pH_{PZC})

The pH at the point of zero charge pH_{PZC} for G/SnO₂ composite was found to be 6.0, obtained by plotting ΔpH versus initial pH values as shown in Fig. 3d. The surface of composite was observed to be negatively charged above the pH_{PZC} (6.0) value. So, the adsorption of anionic dyes like

CR by G/SnO₂ composite can be more efficient at lower pH, while cationic dyes can be adsorbed preferably at pH values higher than 6.0.

Adsorption protocol

Effect of pH

Solution pH is the most important parameter that could obviously affect uptake of adsorbate species on adsorbent surface. Solution pH can alter both, adsorbent surface charge and chemistry of adsorbate molecule (Ali et al. 2019). In this study, removal of CR by G/SnO₂ composite was studied in the pH range of 2–12 at 298 K with initial CR dye

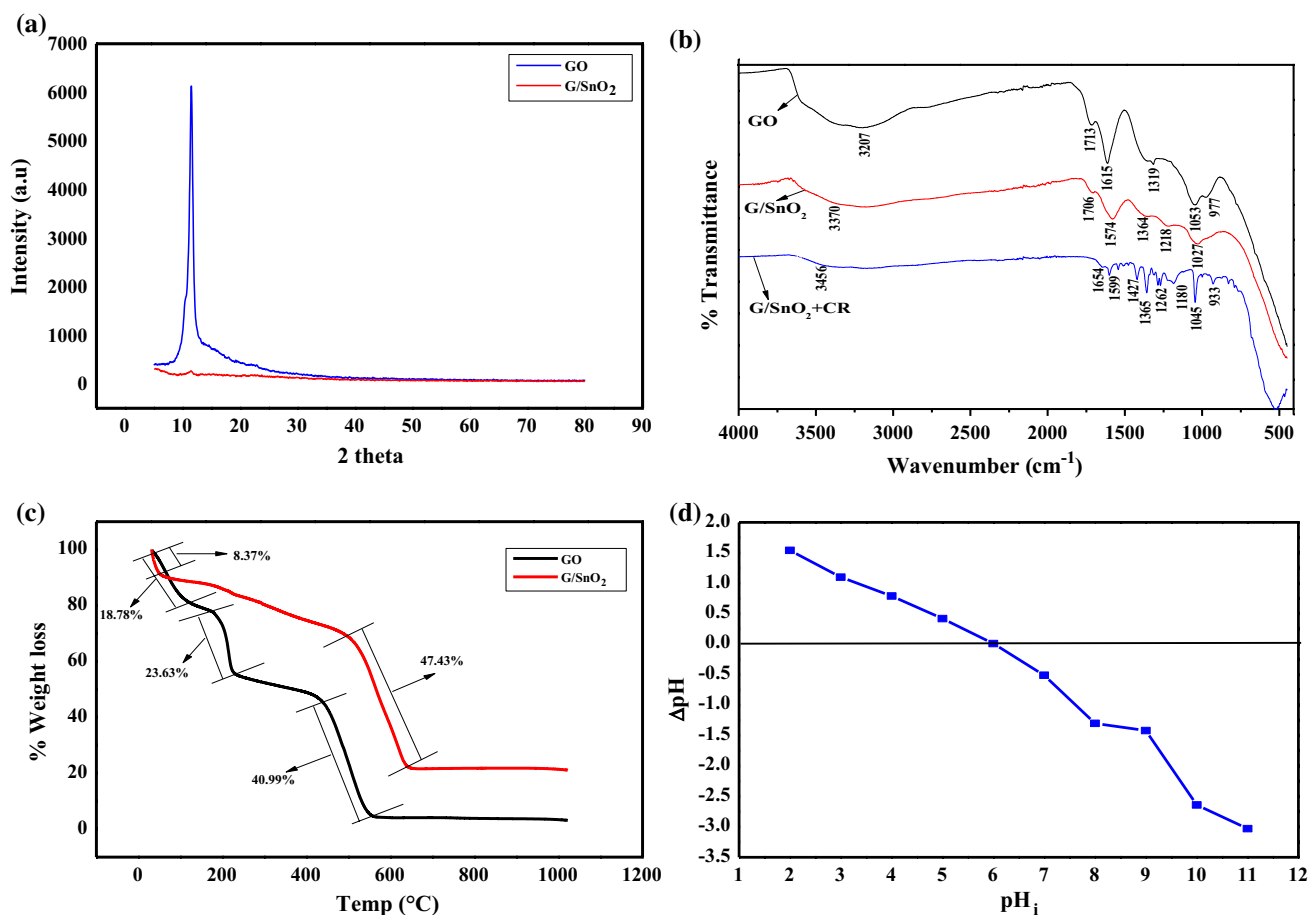


Fig. 3 **a** XRD pattern, **b** FTIR spectra before and after CR adsorption, **c** TGA/DTA curves of GO and G/SnO₂ composite and **d** plot of ΔpH versus pH_i for the determination of pH_{PZC}

concentration of 50 mg/L as shown in Fig. 4a. It can be seen that CR removal efficiency decreases with increasing solution pH. In acidic conditions (pH 2–4) adsorption efficiency was highest (99.11–98.81%) and lowest (13.23%) in basic conditions (pH 12). This phenomenon can be explained on the basis of pH_{PZC} of G/SnO₂ which is 6.0. At pH value lower than 6.0, positive charges are more dominant on the surface of G/SnO₂ composite due to protonation which results in high adsorption of anionic dye CR, controlled by electrostatic interactions arising among negatively charged dye anions and the positive charges on G/SnO₂ surface. However, at pH value beyond pH_{PZC} , G/SnO₂ surface gets deprotonated leading to decrease in percent adsorption. Similar results have been reported by Bhat et al. (2020) in the adsorption of CR by polyvinyl alcohol/melamine–formaldehyde composite.

Effect of CR initial concentration

The impact of initial concentration on the adsorption of CR by G/SnO₂ composite was scrutinized by varying dye

concentration from 20 to 1000 mg/L at pH 3.0 and the results acquired are given in Fig. 4b. It can be seen that the CR uptake capacity first upsurges with rise in concentration of CR molecules from 20 to 1000 mg/L and finally reaches the peak values which then level off after attaining equilibrium, where no more adsorption occurs. Initially, the increase in CR adsorption is associated with the development of driving force that overcomes all mass transfer resistance arising among the existing binding sites on G/SnO₂ surface and CR molecules in solution. The leveling and smoothing of the curves indicate that the available binding site on G/SnO₂ surface gets saturated with CR anions and no further adsorption could occur. Similar investigations were reported by Li and Lin (2019) and Zhao et al. (2017) for the adsorption of CR using La/MFA composite and nickel-based metal–organic framework/graphene oxide composites, respectively.

Effect of contact time and temperature

The influence of shaking duration and temperature on the uptake of CR (initial concentration 700 mg/L) by G/

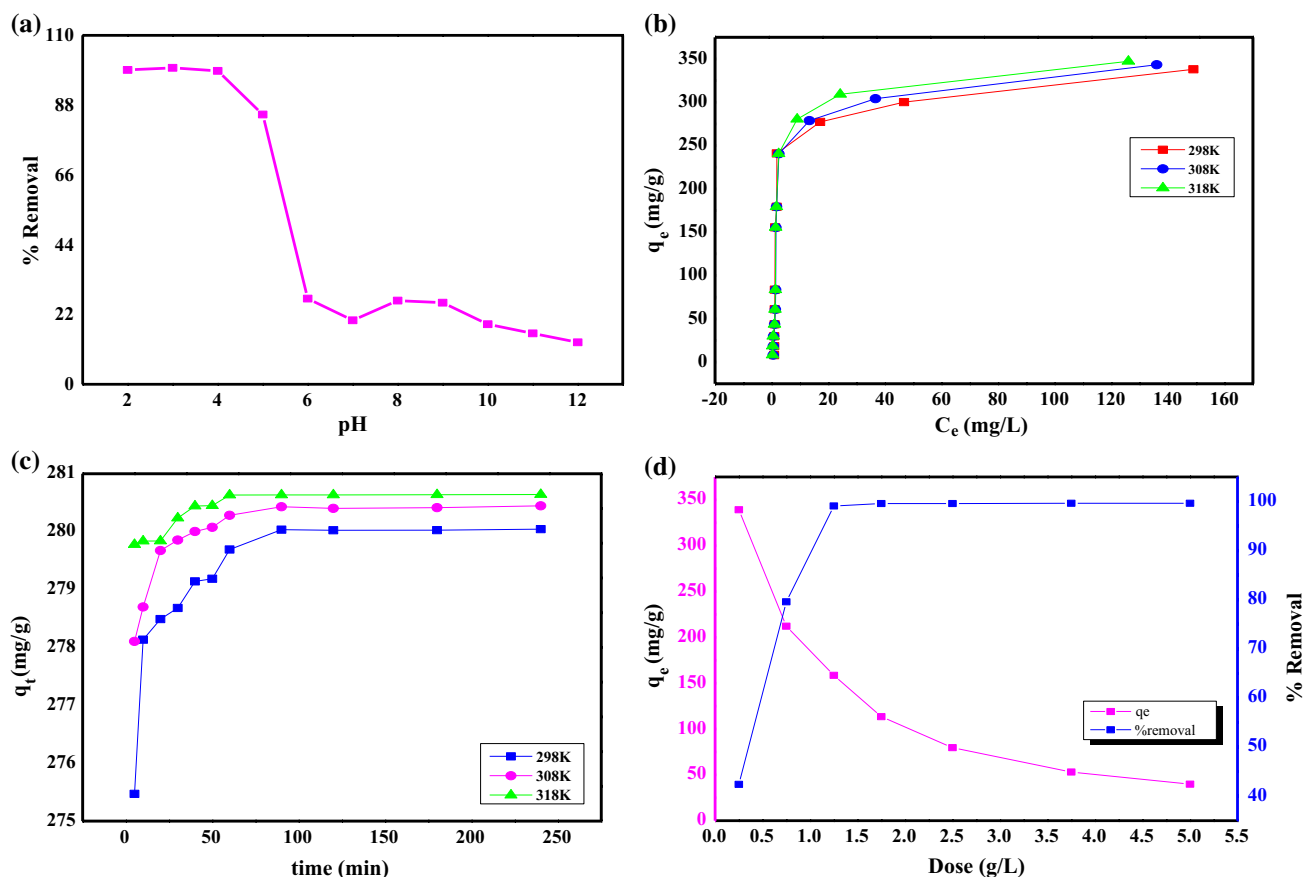


Fig. 4 Effect of **a** dye solution pH, **b** initial concentration, **c** contact time and temperature and **d** adsorbent dose on CR adsorption by G/SnO₂ composite

SnO₂ composite was studied at three different temperatures (298, 303 and 308 K) with dye solution pH 3.0. The results obtained (Fig. 4c) shows that shaking duration has a significant impact on the adsorption of CR. Initially the uptake was fast which then slowly decreased until saturation was achieved. The state of equilibrium was established in about 60 min, which was selected for all other adsorption studies. The enhanced uptake rate at initial intermezzos could be associated with availability of more binding positions on G/SnO₂ surface. These binding positions then start decreasing swiftly with time which leads to slow adsorption rate and eventually attains a constant value. The slow uptake near the saturation point may be because of the electrostatic repulsion among the previously adsorbed CR anions and the dye anions in aqueous phase (Kataria and Garg 2017; Madan et al. 2019). The effect of temperature (298, 308, and 318 K) on CR adsorption can also be seen in Fig. 4c. It can be observed that uptake of CR by G/SnO₂ composite increases with mounting temperature from 298 to 318 K, signifying endothermic nature of CR adsorption. The increase in temperature may facilitate the CR molecules to reach the active sites on adsorbent surface by increasing its solubility. Also, at

elevated temperature the interaction between dye molecule and adsorbent surface increases, leading to high adsorption capacity (Acemioğlu 2004; Zhao et al. 2017).

Effect of adsorbent dose

Adsorbent dose is a highly influential parameter in the adsorption of contaminants from aqueous systems. It explores the uptake capacity of a solid adsorbent material for a particular concentration of an adsorbate. Therefore, optimization of adsorbent dose is very essential for the removal of pollutants from aqueous environments. The impact of adsorbent dosage on the removal of CR with initial concentration of 700 mg/L was assessed by varying the amount of G/SnO₂ composite from 0.01 to 0.2 g at pH 3.0 and 298 K as depicted in Fig. 4d. It can be observed that adsorption efficiency of CR boosts from 42.41 to 99.64% with rising G/SnO₂ mass from 0.01 to 0.2 g. This behavior can be explained by the fact that with increasing adsorbent dose availability of binding sites on G/SnO₂ surfaces increases which leads to high adsorption efficiency. However, the uptake capacity (q_e) decreases with increase in adsorbent



dose due to aggregation of adsorption sites located on surface of adsorbent and reduction in adsorbent-to-adsorbate ratio. Similar results have been reported by other workers for the adsorption of anion and cationic dyes by various adsorbents (Ali et al. 2019; Dandil et al. 2019; Madan et al. 2019).

Equilibrium isotherm studies

To assess the performance of adsorbent during adsorption process and understand the sort of interactions between adsorbate and adsorbent, different adsorption isotherm models were used. In the current study Freundlich, Langmuir and Temkin isotherm models were employed for interpretation of experimentally obtained equilibrium data for CR adsorption on G/SnO₂ composite.

Freundlich isotherm model is one of the earliest known models that describe the sorption mechanism. The fitted plots of Freundlich isotherm model for CR adsorption by G/SnO₂ are given in Fig. 5a. It can be observed from the figure that the isotherms are linear but with very low regression coefficient value ($R^2 \leq 0.67$), indicating that

Freundlich model is not appropriate for describing the equilibrium data under the given experimental conditions. The Freundlich isotherm constants ($1/n$ and K_F) calculated from the slope and intercept of $\ln C_e$ versus $\ln q_e$ plots (Table 2) gives information about the nature and feasibility of sorption process. The value of K_F increases with rising temperature from 298 to 318 K, suggesting endothermic nature of CR adsorption onto G/SnO₂ composite. Furthermore, the $1/n$ values were smaller than 1.0 (Table 2), signifying favorable adsorption process and high affinity of G/SnO₂ composite toward the targeted dye molecules under the given conditions of temperatures.

Langmuir isotherm model plots are presented in Fig. 5b, and the values of model parameters (q_m and K_L) were calculated from the slope and intercept of the linear plots of C_e/q_e versus C_e as summarized in Table 2. The isotherms were linear with high R^2 values (≥ 0.99) than that of Freundlich model. In addition, the experimental and model predicted maximum uptake capacity (q_m , mg/g) are in close agreement. This revealed that the CR dye adsorption by G/SnO₂ composite can be described very well by the Langmuir

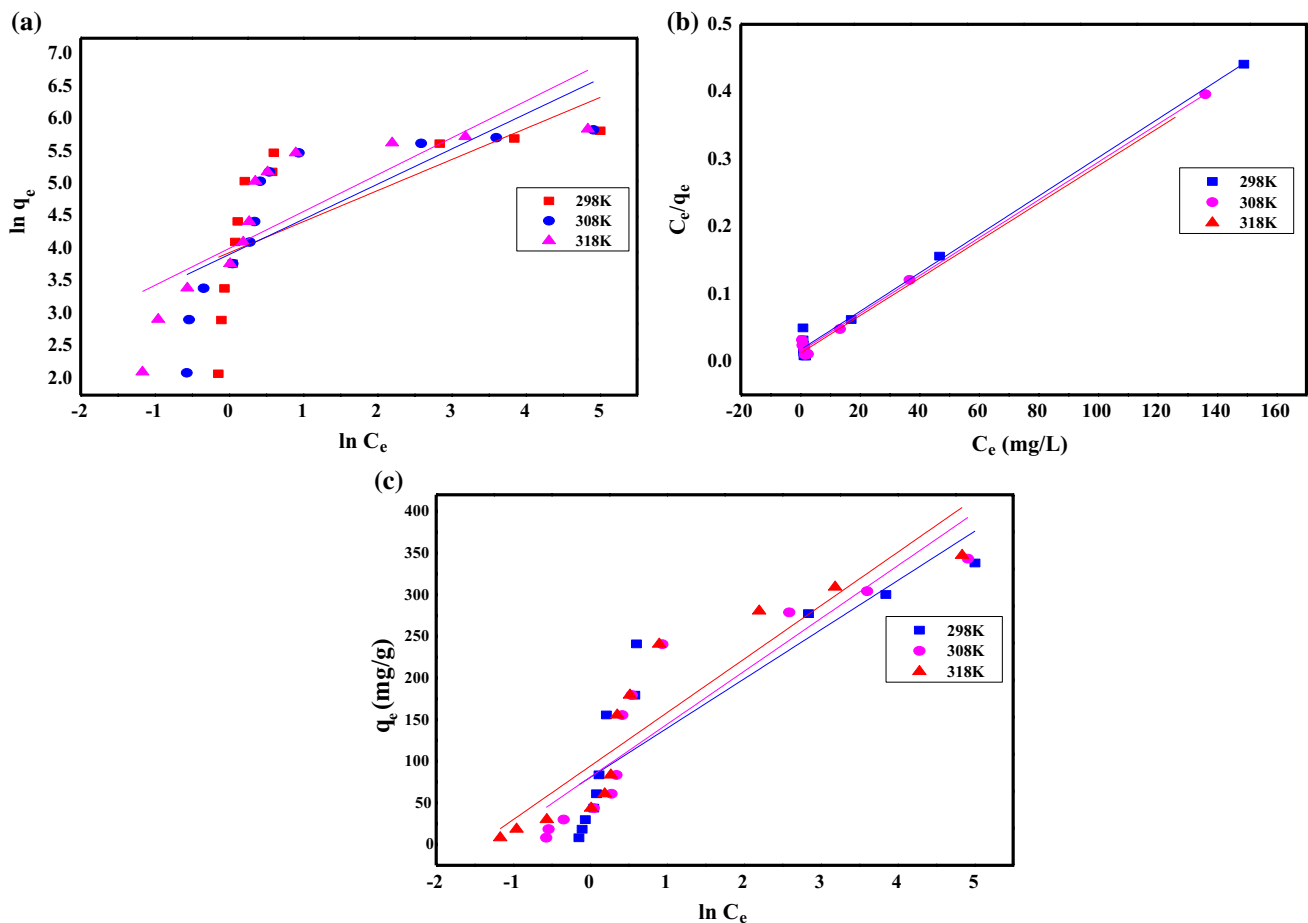


Fig. 5 Plots of **a** Freundlich, **b** Langmuir and **c** Temkin isotherms models for the uptake of CR onto G/SnO₂ composite

Table 2 Different isotherm model parameters for the adsorption of CR by G/SnO₂ composite at three different temperatures

Model	Parameters	Temperature (K)		
		298	308	318
Langmuir	Theoretical q_m (mg/g)	350.87	355.87	359.71
	Experimental q_e (mg/g)	338.07	343.27	347.28
	K_b (L/mg)	0.17	0.20	0.24
	R^2	0.99	0.99	0.99
Freundlich	K_F (mg/g(L/mg) ^{1/m})	50.19	51.62	55.12
	n	2.09	1.84	1.76
	R^2	0.48	0.60	0.67
Temkin	B_T	59.15	63.51	64.25
	b_T (J/mol)	41.88	40.32	41.15
	A_T (L/mg)	3.89	3.57	4.32
	R^2	0.76	0.84	0.65

model, indicating homogeneous nature of G/SnO₂ surface and monolayer sorption process. The monolayer adsorption capacity (q_m) and binding energy constant (K_L , L/mg) values increases from 350.87 to 359.71 mg/g and from 0.17 to 0.24 L/mg, respectively, with rising temperature from 298 to 318 K (Table 2), confirmed endothermic nature CR adsorption. The favorability of adsorption process and fitting quality of Langmuir isotherm model was further assessed using separation factor (R_L). The values of R_L at all studied temperatures were found between zero and unity (Table 2), demonstrating feasible adsorption of CR onto G/SnO₂ composite that can be explained by Langmuir model very well. Similar findings have been reported by Parida and Pradhan (2010) for the adsorption of phenolic compounds using manganese nodule leached residue as adsorbent.

The values of Temkin isotherm constants, K_T and b_T for the uptake of CR by G/SnO₂ were found from the intercept and slopes of q_e versus $\ln C_e$ plots, respectively (Fig. 5c), and the results are given in Table 2. The smaller value of correlation coefficient ($R^2 \leq 0.76$) showed that Temkin model did not fit the experimental data. With rising dye solution temperature from 298 to 318 K, b_T and K_T values were correspondingly increased from 40.32 to 41.88 J/mol and 3.89 to 4.32 L/mg. This phenomenon could be associated to the increase in surface coverage due to adsorbate–adsorbent interaction and endothermic nature of CR adsorption (Jalil et al. 2012).

Kinetics study

The kinetic and mechanism of CR adsorption by G/SnO₂ was studied at 298, 308 and 318 K using pseudo-first order, pseudo-second order, intra-particle diffusion and Boyd's models. The plots for pseudo-first order, pseudo-second order, intra-particle diffusion and Boyd's models are shown

in Fig. 6a–d and the calculated kinetic parameters are summarized in Table 3. Based on the lower R^2 values, the pseudo-first order model did not fit well the experimental kinetic data of CR adsorption under the given conditions of temperature. However, the plots of t/q_t versus t for pseudo-second order model (Fig. 6b) are linear with very high value of correlation coefficient (equal to unity) fitted very well to the kinetic data points. Additionally, the closeness of model predicted adsorption capacities (q_e , cal) based on pseudo-second order model and experimentally determined values (Table 3) further verified the good fitting quality of pseudo-second order kinetic model at all the studied temperatures. These results revealed that the uptake of CR may be accomplished by electron transfer among the functional groups on G/SnO₂ surface and CR anions via chemical interaction (Nayak and Pal 2017). The pseudo-second order rate constant (k_2) values increases from 0.03 to 0.13 g/mg min, suggesting that the affinity of G/SnO₂ composite toward CR increases with rising temperature from 298 to 318 K, displaying endothermic nature of sorption process. The increase in k_2 values with temperature may be due to the quick transfer of CR molecules from solution to the adsorbent surface at elevated temperature. Other researchers have observed similar results for the adsorption of Congo red dye using TiO₂ nanoparticles and inorganic-and organic-modified kaolinite as adsorbent materials (Shaban et al. 2018; Rath et al. 2019).

To get insight about the rate limiting step and diffusion mechanism of CR adsorption onto G/SnO₂ composite, Weber–Morris intra-particle diffusion model was employed for analyzing the kinetic data. The intra-particle diffusion model parameters (k_i and C) were evaluated from the slope and intercept of linear plots of q_t versus $t^{0.5}$ (Fig. 6c) and are listed in Table 3. It can be observed from the figure that the plot of q_t versus $t^{0.5}$ did not pass through the origin at all studied temperatures and have low regression coefficient values ($R^2 \leq 0.91$), suggesting that only intra-particle diffusion is not the rate controlling step for CR adsorption (Abbas et al. 2017). The boundary layer thickness (C) values were increased from 275.28 to 279.31 mg/g with increasing temperature from 298 to 318 K, suggesting that boundary diffusion effect increases with rising dye solution temperature. The kinetic data were further analyzed via Boyd model to evaluate whether intra-particle diffusion or film diffusion is the rate determining step. The Boyd model plots (Fig. 6d) were found to be linear but did not pass through the origin, confirming that both film diffusion and particle diffusion control the rate of CR adsorption by G/SnO₂ composite.

Thermodynamic investigations

To further understand the impact of solution temperature on CR adsorption by G/SnO₂ composite thermodynamic studies



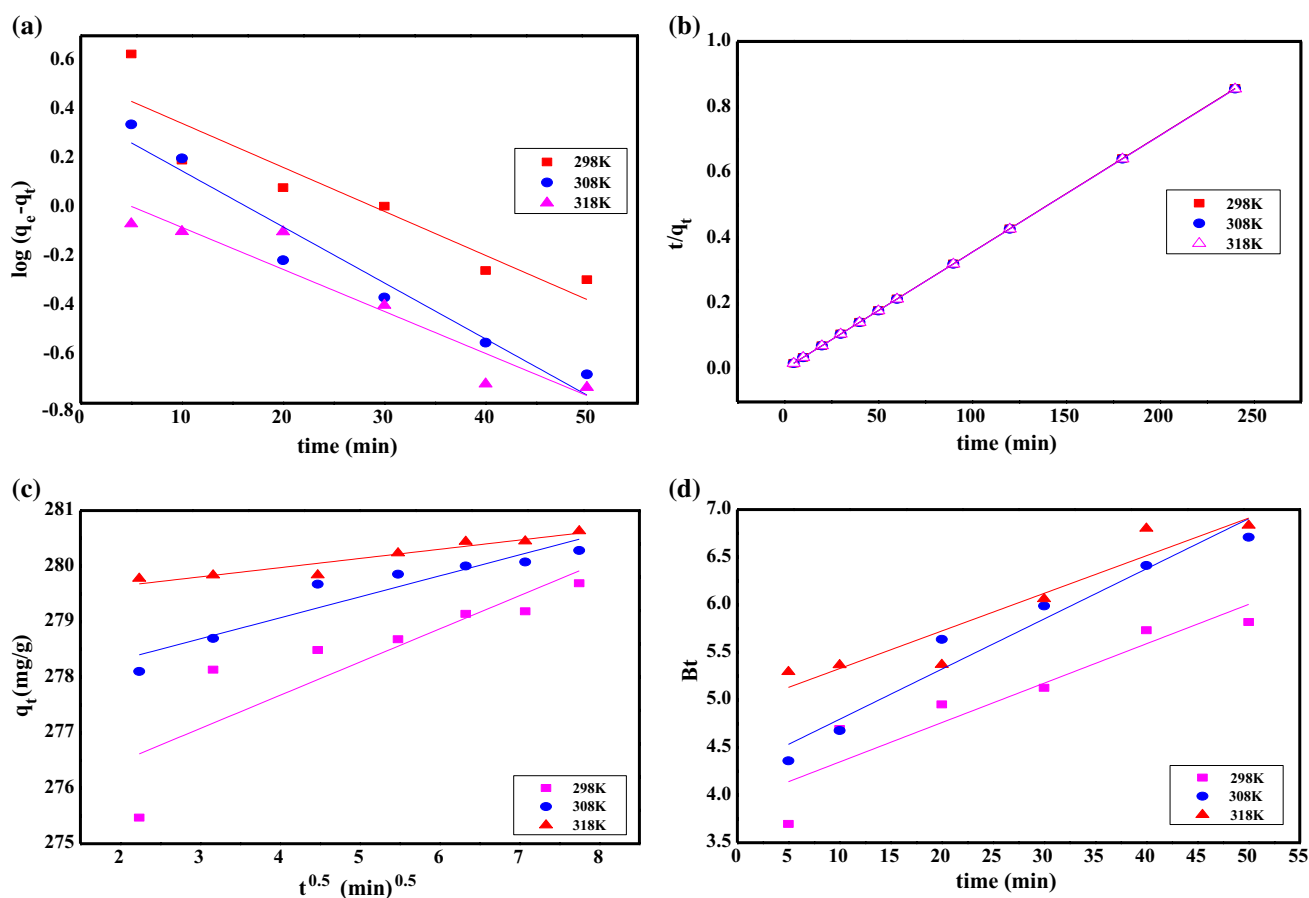


Fig. 6 a Pseudo-first order, b Pseudo-second order, c Intra-particle diffusion and d Boyd model plots for CR adsorption by G/SnO₂ composite

Table 3 Kinetic and intra-particle diffusion model parameters for CR adsorption by G/SnO₂ composite

Model	Parameters	Temperature (K)		
		298	308	318
Pseudo-first order	q_e , cal (mg/g)	3.33	2.38	1.23
	q_e , exp (mg/g)	279.69	280.28	280.63
	k_1 (1/min)	0.04	0.05	0.04
	R^2	0.86	0.95	0.90
Pseudo-second order	q_e , cal (mg/g)	280.11	280.90	280.90
	q_e , exp (mg/g)	280.04	280.44	280.64
	k_2 (g/min mg)	0.03	0.06	0.12
	R^2	1.00	1.00	1.00
Intra-particle diffusion	K_i (mg/g min ^{0.5})	0.59	0.38	0.16
	C (mg/g)	275.28	277.56	279.31
	R^2	0.77	0.90	0.91

were carried out at three different temperatures (298, 308 and 318 K). Different thermodynamic parameters like ΔH° , ΔG° and ΔS° were used to evaluate the intrinsic energetic changes associated with CR adsorption. The ΔS° and ΔH°

were found from the intercept and slopes of the linear plot of $\ln K_L$ versus $1/T$ (Fig. 7) and the results achieved are compiled in Table 4. The positive value of ΔH° has shown endothermic nature of sorption process, while positive value of ΔS° revealed increase randomness at solid–liquid interface due to high affinity of G/SnO₂ composite for CR dye in acidic pH ranges. Additionally, the negatively values of ΔG° have shown spontaneous and favorable adsorption of CR by G/SnO₂ composite at all the studied temperatures. The decrease in ΔG° value (Table 4) with increasing temperature further verified that the feasibility of sorption process increases with temperature which is in agreement with results obtained from isotherm studies. Kumara et al. reported similar findings for the adsorption crystal violet using TLAC/Chitosan composite (Kumari et al. 2017). Moreover, the magnitude of activation energy (E_a) also gives valuable information about the nature of adsorption process. For physical adsorption its range is from 4–40 kJ/mol and for chemisorption it is 40–800 kJ/mol (Kaur et al. 2015). The E_a value calculated for CR adsorption onto G/SnO₂ at three different temperatures (298, 308 and 318 K) using Arrhenius equation was found to be 54.59 kJ/mol exposed that

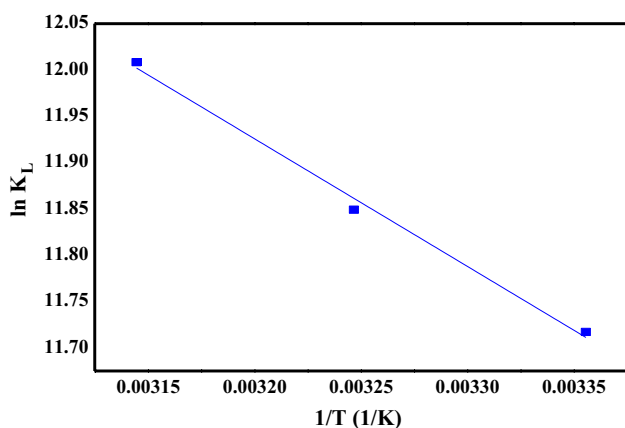


Fig. 7 Plot of $\ln K_L$ versus $1/T$ for CR uptake by G/SnO_2 composite

Table 4 Various thermodynamic parameters for CR adsorption by G/SnO_2 composite

T (K)	ΔG° (kJ/mol)	ΔH° (kJ/mol)	ΔS° (J/mol K)	E_a (kJ/mol)
298	-29.02	11.46	135.82	54.59
308	-30.37			
318	-31.73			

the adsorption process in the present case is chemisorption. Similar investigations have been reported by other workers for cationic and anionic dyes adoption using different adsorbents (Abbas et al. 2017; Gemici et al. 2020).

Desorption and adsorbent regeneration

Desorption and regeneration studies were carried out to assess the possible reuse of adsorbent and feasibility of the process. In regeneration experiments, choice of eluent is a top priority step as eluents can weaken the attractive forces among dyes molecules and adsorbent surface which is possible by a specific eluent only. In the current study, HCl (0.1 M), DDW, ethanol and NaOH (0.1 M) were used as eluents and maximum desorption of CR (93.03%) from the surface of G/SnO_2 composite was achieved with 0.1 M NaOH solution as can be seen in Fig. 8a. Hence, NaOH solution was selected for further regeneration studies. The highest desorption in alkaline medium may be due to the deprotonation of G/SnO_2 surface leading to a reduction in electrostatic interactions among dye anions and adsorbent surface.

Regeneration of dye loaded adsorbent was inspected in five consecutive adsorption–desorption cycles using NaOH (0.1 M) as desorbing medium and the results obtained are illustrated in Fig. 8b. From the figure it can be seen that the G/SnO_2 composite adsorption efficiency slightly fall after each cycle but is still higher than 75% even in the fifth cycle,

shown that G/SnO_2 composite could be recycled many times for dyes containing wastewater without any substantial loss in sorption efficiency. The slight reduction in uptake efficiency in the successive cycles may be due to loss of some active sites on G/SnO_2 composite surface (Hosseini et al. 2011).

Comparison with other adsorbent

The maximum monolayer uptake capacity of G/SnO_2 composite for CR was compared with many other already reported adsorbents, as illustrated in Table 5. It can be perceived from the table that G/SnO_2 composite has considerably high uptake capacity for CR than many other previously reported adsorbents. This confirmed that G/SnO_2 composite synthesized by solvothermal method could be an efficient adsorbent for detoxification of highly toxic anionic dyes, such as CR from aqueous environment.

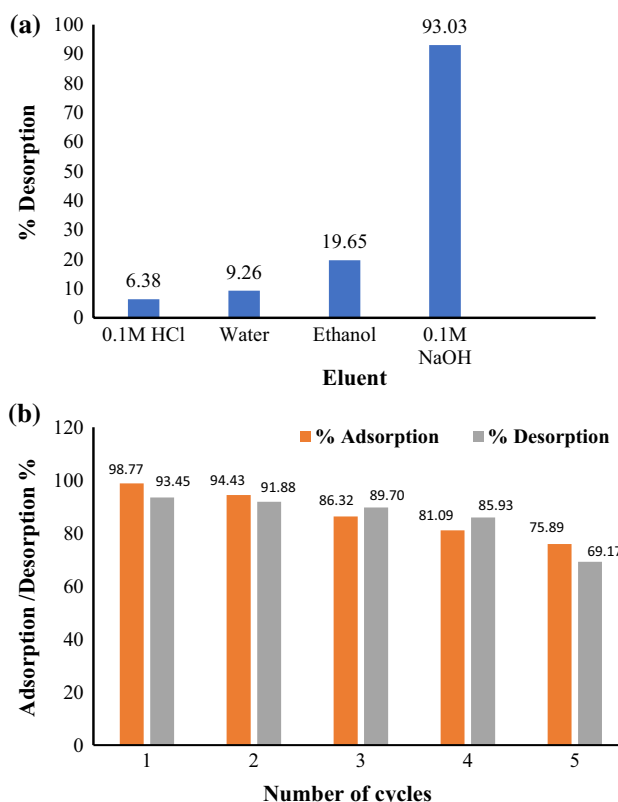


Fig. 8 a Impact of eluents type on CR desorption and b regeneration of G/SnO_2 composite in five consecutive cycles

Table 5 Comparison of monolayer uptake capacity of G/SnO₂ for CR with other reported adsorbents

Adsorbents	q_m (mg/g)	References
Cationic surfactant modified (SMC)	200.00	Nodehi et al. (2020)
Unmodified clinoptilolite (NC) and Walnut shell (WS)	16.92	Nodehi et al. (2020)
	84.00	Liu et al. (2019b)
Hypercross-linked,3,5-diacrylamidobenzoic acid-based resin (APEADA)	280.00	Waheed et al. (2019)
Chemically modified egg shell	117.65	Parvin et al. (2019)
Silanized and aminated lignin (SAL)	74.40	An et al. (2020)
Hierarchically processed pineapple peel hydrogels	114.94	Dai et al. (2020)
Pineapple peel carboxymethyl cellulose-g-poly (acrylic acid-co-acrylamide)/graphene oxide hydrogels	23.67	Dai et al. (2019)
Sargassum fusiforme-activated carbon	234.00	Ma et al. (2020)
Polyacrolein (PA)	51.80	Tang et al. (2020)
Graphene tin oxide (G/SnO ₂) composite	359.71	Present study

Conclusion

Graphene tin oxide (G/SnO₂) composite was successfully synthesized by a simple solvothermal method and was used efficiently for the removal of toxic anionic dye, CR, from aqueous environment. EDX analysis presented a high percentage of Sn (62.11%), accompanied by decrease in percentage of carbon (from 47.45 to 13.75%) and oxygen (from 39.37 to 23.71%) confirmed that G/SnO₂ composite has been successfully prepared which is also supported by FTIR analysis. TGA analysis has showed that G/SnO₂ composite is thermally more stable than GO as decomposition of its carbon skeleton occurred in the temperature range of 480–650 °C, which is much higher than that of graphene oxide (430–550 °C). The p*H*_{PCZ} (6.0) of G/SnO₂ has shown that it can efficiently remove both anionic (below pH 6.0) and cationic (above pH 6.0) dyes from aqueous solutions. Highest adsorption of CR was observed in the pH range of 2–5. Adsorption of CR was explained very well by Langmuir isotherm model and pseudo-second order kinetic model with the maximum monolayer adsorption capacity 359.71 mg/g at 318 K which is quite high than many other adsorbent already reported adsorbents. Thermodynamic study has shown endothermic and spontaneous nature of CR adsorption onto G/SnO₂. Regeneration analyses shown that G/SnO₂ composite can be used many times for the adsorption of azo dyes from wastewater without any significant loss in sorption efficiency.

Acknowledgements The authors of the present paper are thankful to the Director National Center of Excellence in Physical Chemistry, University of Peshawar, Pakistan, for providing the support and all facilities to accomplish the research project.

Funding This research work did not receive any specific grant from funding agencies.

Availability of data and material The datasets used and/or analyzed during the current study are available from the corresponding author on reasonable request.

Code availability Not applicable.

Declarations

Conflicts of interest The authors declare that they have no competing interest.

Ethics approval Not applicable.

Consent to participate Not applicable.

Consent for publication Not applicable.

References

- Abbas AM, Mohammed YI, Himdan TA (2017) Adsorption kinetic and thermodynamic study of congo red dye on synthetic zeolite and modified synthetic zeolite. *Ibn AL-Haitham J Pure Appl Sci* 28:54–72
- Abbasi S (2020) Adsorption of dye organic pollutant using magnetic ZnO embedded on the surface of graphene oxide. *J Inorg Organomet Polym Mater* 30:1924–1934
- Acemioğlu B (2004) Adsorption of Congo red from aqueous solution onto calcium-rich fly ash. *J Colloid Interface Sci* 274:371–379
- Alam SN, Sharma N, Kumar L (2017) Synthesis of graphene oxide (GO) by modified hummers method and its thermal reduction to obtain reduced graphene oxide (rGO). *Graphene* 6:1–18
- Ali R, Mahmood T, Din SU, Naeem A, Aslam M, Farooq M (2019) Efficient removal of hazardous malachite green dye from aqueous solutions using H₂O₂ modified activated carbon as potential low-cost adsorbent: kinetic, equilibrium, and thermodynamic studies. *Desalin Water Treat* 151:167–182
- Ali R, Mahmood T, Naeem A, Ullah A, Aslam M, Khan S (2021) Process optimization of Auramine O adsorption by



- surfactant-modified activated carbon using Box–Behnken design of response surface methodology. *Desalin Water Treat* 217:367–390
- Aliabadi RS, Mahmoodi NO (2018) Synthesis and characterization of polypyrrole, polyaniline nanoparticles and their nanocomposite for removal of azo dyes; sunset yellow and Congo red. *J Clean Prod* 179:235–245
- Al-Othman ZA, Ali R, Naushad M (2012) Hexavalent chromium removal from aqueous medium by activated carbon prepared from peanut shell: adsorption kinetics, equilibrium and thermodynamic studies. *Chem Eng J* 184:238–247
- An L, Si C, Bae JH, Jeong H, Kim YS (2020) One-step silanization and amination of lignin and its adsorption of Congo red and Cu (II) ions in aqueous solution. *Int J Biol Macromol* 159:222–230
- Basheer AA (2018) New generation nano-adsorbents for the removal of emerging contaminants in water. *J Mol Liq* 261:583–593
- Bharath G, Alhseinat E, Ponpandian N, Khan MA, Siddiqui MR, Ahmed F, Alsharaeh EH (2017) Development of adsorption and electrosorption techniques for removal of organic and inorganic pollutants from wastewater using novel magnetite/porous graphene-based nanocomposites. *Sep Purif Technol* 188:206–218
- Bhat SA, Zafar F, Mondal AH, Mirza AU, Haq QMR, Nishat N (2020) Efficient removal of Congo red dye from aqueous solution by adsorbent films of polyvinyl alcohol/melamine-formaldehyde composite and bactericidal effects. *J Clean Prod* 255:120062
- Boyd G, Adamson A, Myers L Jr (1947) The exchange adsorption of ions from aqueous solutions by organic zeolites. II. Kinetics. *J Am Chem Soc* 69:2836–2848
- Corbett JF (1972) Pseudo first-order kinetics. *J Chem Educ* 49:663
- Dai H, Zhang Y, Ma L, Zhang H, Huang H (2019) Synthesis and response of pineapple peel carboxymethyl cellulose-g-poly (acrylic acid-co-acrylamide)/graphene oxide hydrogels. *Carbohydr Polym* 215:366–376
- Dai H, Huang Y, Zhang H, Ma L, Huang H, Wu J, Zhang Y (2020) Direct fabrication of hierarchically processed pineapple peel hydrogels for efficient Congo red adsorption. *Carbohydr Polym* 230:115599
- Dandil S, Sahbaz DA, Acikgoz C (2019) High performance adsorption of hazardous triphenylmethane dye-crystal violet onto calcinated waste mussel shells. *Water Qual Res J* 54:249–256
- Dbik A, Bentahar S, El Khomri M, El Messaoudi N, Lacherai A (2020) Adsorption of Congo red dye from aqueous solutions using tunics of the corm of the saffron. *Mater Today: Proceed* 22:134–139
- Deng L, Zeng H, Shi Z, Zhang W, Luo J (2018) Sodium dodecyl sulfate intercalated and acrylamide anchored layered double hydroxides: a multifunctional adsorbent for highly efficient removal of Congo red. *J Colloid Interface Sci* 521:172–182
- Dhanabalan A, Li X, Agrawal R, Chen C, Wang C (2013) Fabrication and characterization of SnO₂/Graphene composites as high capacity anodes for Li-ion batteries. *Nanomaterials* 3:606–614
- Freundlich H (1907) Über die adsorption in lösungen. *Z Phys Chem* 57(1):385–470
- Gemici BT, Uzun Ozel H, Ozel HB (2020) Adsorption behaviors of crystal violet from aqueous solution using Anatolian black pine (*Pinus nigra* Arnold.): kinetic and equilibrium studies. *Sep Sci Technol* 55:406–414
- Golmohammadi F, Hazrati M, Safari M (2019) Removal of reactive yellow 15 from water sample using a magnetite nanoparticles coated with covalently immobilized dimethyl octadecyl [3-(trimethoxysilylpropyl)] ammonium chloride ionic liquid. *Microchem J* 144:64–72
- Hassan AM, Ibrahim WAW, Bakar MB, Sanagi MM, Sutirman ZA, Nodeh HR, Mokhter MA (2020) New effective 3-aminopropyltrimethoxysilane functionalized magnetic sporopollenin-based silica coated graphene oxide adsorbent for removal of Pb (II) from aqueous environment. *J Environ Manage* 253:109658
- Ho Y-S (2006) Review of second-order models for adsorption systems. *J Hazard Mater* 136:681–689
- Hosseini S, Khan MA, Malekbala MR, Cheah W, Choong TS (2011) Carbon coated monolith, a mesoporous material for the removal of methyl orange from aqueous phase: adsorption and desorption studies. *Chem Eng J* 171:1124–1131
- Hua H, Liub J, Xub Z, Zhanga L, Chenga B, Ho W (2019) Hierarchical porous Ni/Co-LDH hollow dodecahedron with excellent adsorption property for Congo red and Cr(VI) ions. *Appl Surf Sci* 478:981–990
- Jalil A, Triwahyono S, Yaakob M, Azmi Z, Sapawe N, Kamarudin N, Setiabudi H, Jaafar N, Sidik S, Adam S (2012) Utilization of bivalve shell-treated *Zea mays* L. (maize) husk leaf as a low-cost biosorbent for enhanced adsorption of malachite green. *Bioresour Technol* 120:218–224
- Jiao C, Xiong J, Tao J, Xu S, Zhang D, Lin H, Chen Y (2016) Sodium alginate/graphene oxide aerogel with enhanced strength–toughness and its heavy metal adsorption study. *Int J Biol Macromol* 83:133–141
- Kataria N, Garg V (2017) Removal of Congo red and Brilliant green dyes from aqueous solution using flower shaped ZnO nanoparticles. *J Environ Chem Eng* 5:5420–5428
- Kaur S, Rani S, Mahajan RK (2015) Adsorption of dye crystal violet onto surface-modified *Eichhornia crassipes*. *Desalin Water Treat* 53:1957–1969
- Kumari HJ, Krishnamoorthy P, Arumugam T, Radhakrishnan S, Vasudevan D (2017) An efficient removal of crystal violet dye from waste water by adsorption onto TLAC/Chitosan composite: a novel low cost adsorbent. *Int J Biol Macromol* 96:324–333
- Langmuir I (1916) The constitution and fundamental properties of solids and liquids. Part I. Solids *J Am Chem Soc* 38:2221–2295
- Li BG, Lin XH (2019) Adsorption of Congo red from aqueous solution using La/MFA composite as adsorbent. *Mater Sci Forum Trans Tech Publ* 944:1117–1122
- Lin Q, Li Y, Yang M (2012) Tin oxide/graphene composite fabricated via a hydrothermal method for gas sensors working at room temperature. *Sens Actuators b: Chem* 173:139–147
- Liu C, Liu H, Zhang K, Dou M, Pan B, He X, Lu C (2019a) Partly reduced graphene oxide aerogels induced by proanthocyanidins for efficient dye removal. *Bioresour Technol* 282:148–155
- Liu M, Li X, Du Y, Han R (2019b) Adsorption of methyl blue from solution using walnut shell and reuse in a secondary adsorption for Congo red. *Bioresour Technol Rep* 5:238–242
- Ma M, Ying H, Cao F, Wang Q, Ai N (2020) Adsorption of Congo red on mesoporous activated carbon prepared by CO₂ physical activation. *Chin J Chem Eng* 28:1069–1076
- Madan S, Shaw R, Tiwari S, Tiwari SK (2019) Adsorption dynamics of Congo red dye removal using ZnO functionalized high silica zeolitic particles. *Appl Surf Sci* 487:907–917
- Mahmood T, Ali R, Naeem A, Hamayun M, Aslam M (2017) Potential of used *Camellia sinensis* leaves as precursor for activated carbon preparation by chemical activation with H₃PO₄; optimization using response surface methodology. *Process Saf Environ Prot* 109:548–563
- Mahmood T, Aslam M, Naeem A, Ali R, Saddique T (2018) Equilibrium, kinetics, mechanism and thermodynamics studies of As (III) adsorption from aqueous solution using iron impregnated used tea. *Desalin Water Treat* 104:135–148
- Mohammadi A, Doctorsafaei AH, Zia KM (2018) Alginate/calix [4] arenes modified graphene oxide nanocomposite beads: Preparation, characterization, and dye adsorption studies. *Int J Biol Macromol* 120:1353–1361



- Naushad M, Alqadami AA, AlOthman ZA, Alsohaimi IH, Algamdi MS, Aldawsari AM (2019a) Adsorption kinetics, isotherm and reusability studies for the removal of cationic dye from aqueous medium using arginine modified activated carbon. *J Mol Liq* 293:111442
- Naushad M, Sharma G, AlOthman ZA (2019b) Photodegradation of toxic dye using Gum Arabic-crosslinked-poly (acrylamide)/Ni (OH) 2/FeOOH nanocomposites hydrogel. *J Clean Prod* 241:118263
- Nayak AK, Pal A (2017) Green and efficient biosorptive removal of methylene blue by *Abelmoschus esculentus* seed: process optimization and multi-variate modeling. *J Environ Manage* 200:145–159
- Nodehi R, Shayesteh H, Kelishami AR (2020) Enhanced adsorption of congo red using cationic surfactant functionalized zeolite particles. *Microchem J* 153:104281
- Parida K, Pradhan AC (2010) Removal of phenolic compounds from aqueous solutions by adsorption onto manganese nodule leached residue. *J Hazard Mater* 173(1–3):758–764
- Parvin S, Biswas BK, Rahman MA, Rahman MH, Anik MS, Uddin MR (2019) Study on adsorption of Congo red onto chemically modified egg shell membrane. *Chemosphere* 236:124326
- Rath P, Priyadarshini B, Behera S, Parhi P, Panda S, Sahoo T (2019) Adsorptive removal of Congo Red dye from aqueous solution using TiO₂ nanoparticles: kinetics, thermodynamics and isothermal insights. *AIP Conf Proc* 2115:030115
- Shaban M, Sayed MI, Shahien MG, Abukhadra MR, Ahmed ZM (2018) Adsorption behavior of inorganic-and organic-modified kaolinite for Congo red dye from water, kinetic modeling, and equilibrium studies. *J Sol-Gel Sci Technol* 87:427–441
- Shahriary L, Athawale AA (2014) Graphene oxide synthesized by using modified hummers approach. *Int J Renew Energy Environ Eng* 2:58–63
- Sun H, Cao L, Lu L (2011) Magnetite/reduced graphene oxide nanocomposites: one step solvothermal synthesis and use as a novel platform for removal of dye pollutants. *Nano Res* 4:550–562
- Tang J, Zhang Y-F, Liu Y, Li Y, Hu H (2020) Efficient ion-enhanced adsorption of congo red on polyacrolein from aqueous solution: experiments, characterization and mechanism studies. *Sep Purif Technol* 252:117445
- Temkin M, Pyzhev V (1940) Recent modifications to Langmuir isotherms, pp 217–222
- Waheed A, Mansha M, Kazi IW, Ullah N (2019) Synthesis of a novel 3, 5-diacrylamidobenzoic acid based hyper-cross-linked resin for the efficient adsorption of Congo Red and Rhodamine B. *J Hazard Mater* 369:528–538
- Weber TW, Chakravorti RK (1974) Pore and solid diffusion models for fixed-bed adsorbers. *AIChE J* 20:228–238
- Weber WJ, Morris JC (1963) Kinetics of adsorption on carbon from solution. *J Sanit Eng Div* 89:31–60
- Wekoye JN, Wanyonyi WC, Wangila PT, Tonui MK (2020) Kinetic and equilibrium studies of Congo red dye adsorption on cabbage waste powder. *Environ Chem Ecotoxicol* 2:24–31
- Wu J, Shen X, Jiang L, Wang K, Chen K (2010) Solvothermal synthesis and characterization of sandwich-like graphene/ZnO nanocomposites. *Appl Surf Sci* 256:2826–2830
- Yang J-Y, Jiang X-Y, Jiao F-P, Yu J-G (2018) The oxygen-rich pentaerythritol modified multi-walled carbon nanotube as an efficient adsorbent for aqueous removal of alizarin yellow R and alizarin red S. *Appl Surf Sci* 436:198–206
- Zhang C, Peng X, Guo Z, Cai C, Chen Z, Wexler D, Li S, Liu H (2012) Carbon-coated SnO₂/graphene nanosheets as highly reversible anode materials for lithium ion batteries. *Carbon* 50:1897–1903
- Zhao S, Chen D, Wei F, Chen N, Liang Z, Luo Y (2017) Removal of Congo red dye from aqueous solution with nickel-based metal-organic framework/graphene oxide composites prepared by ultrasonic wave-assisted ball milling. *Ultrason Sonochem* 39:845–852

